Chromia Pillaring in α-Zirconium Phosphate: A Structural Investigation Using X-Ray Absorption Spectroscopy

Deborah J. Jones,[†] Jacques Rozière,*[,†] Pedro Maireles-Torres,[†] Antonio Jiménez-López,[‡] Pascual Olivera-Pastor,[‡] Enrique Rodríguez-Castellón,[‡] and Anthony A. G. Tomlinson[§]

Laboratoire des Agrégats Moléculaires et Matériaux Inorganiques, URA CNRS 79, Université Montpellier 2, 34095 Montpellier cédex 5, France, Departamento de Quimica Inorganica, Cristalografia y Mineralogia, Universidad de Malaga, 29071 Malaga, Spain, and Istituto di Chimica dei Materiali, CNR, Monterotondo Stazione, 00016 Rome, Italy

Received February 15, 1995[⊗]

An X-ray absorption spectroscopic (XAS) study has been carried out on the intercalated precursor polyhydroxy(acetato)chromium(III) α-zirconium phosphates, a chromia-pillared derivative obtained by calcination at 400 °C, and the amorphous congener obtained after calcination at 800 °C. The precursor solids contain interlayer hydroxy−Cr^{III} clusters with connnectivities of a flat dimer (12 Å phase), a closed trimer (17 Å phase), an open tetramer (34 Å phase), and also contain a 25 Å phase with connectivity between trimer and tetramer. The acetate residues little influence the XAFS analysis, and orientations of the cluster species present between the layers are suggested on the basis of double-layer structures. The chromia-pillared material obtained after calcination of the 34 Å phase has a ribbonlike structure comprising pseudo-octahedral [$Cr^{III}O_6$] units showing Cr- - -P distances (3.25 Å), as expected for coordination of the pillar to the phosphate layer. There is no evidence for Cr^{VI} formation, unlike the oxidation that occurs on calcination in montmorillonite analogues. Amorphization at 800 °C causes rearrangement, and the pillar is best described as a corner-shared oxide−phosphate nanoparticle with contributions from bidentate PO_4^{3-} groups. The implications for the thermal stability of oxide-pillared materials prepared using current pillaring methods are discussed.

Introduction

Inducing anisotropic porosity into layered materials *via* pillaring techniques[1] has, over the past 10 years, been concerned mainly with alumina and silica pillaring.[2] However, in early work in the field attention was also turned to transition metal complexes, especially chromia-pillared smectites,[3] many of which have been shown to be of some interest as dehydrogenation and selective oxidation catalysts.[3,4] More recently, colloid methods have been utilized to produce chromia-pillared materials from the well-established group IV layered phosphates, which demonstrate improved pore homogeneity.[5] In common with many other pillared materials[6] only very indirect information is available on the oxide-pillar structure adopted after calcination of precursor species, because the type of ordering present precludes the use of standard X-ray diffraction methods. One means of recourse is to utilise extended X-ray absorption fine structure (XAFS) techniques, as in a recent study of the insertion of hydroxyoxychromium(III) cations into a bentonite,[7] from which it was concluded that the chromia pillars formed after calcination at 250 °C consisted of mixed valence $Cr^{III}Cr^{VI}$ species. This conclusion is different from that reached, *via* indirect spectroscopic methods, for chromia-pillared phosphates,[8] which prompts us to report a detailed XAFS study of the latter. The aims are to (i) identify and assign local connectivities of polyhydroxychromium-intercalated precursors with stepwise changes in interlayer spacing and (ii) define the oxidation state and geometry of the nano-chromia particles obtained after calcination. The overall objective is to throw light on both the surface chemistry of the precursor intercalation stage and how this relates to oxide-pillar formation and identify the structural changes they undergo on high-temperature calcination.

Experimental Section

Materials. Polyhydroxychromium(III)-intercalated precursors α-zirconium phosphates were prepared by contacting *n*-propylamine−α-zirconium phosphate suspensions with $Cr(OAc)_3$ aqueous solutions of differing chromium concentrations (8.78−181.27 mequiv of Cr^{3+} added /g of ZrP_2O_7; see ref 8 for details). After being refluxed for 4 days, the suspensions were centrifuged and the solids separated, washed well with water, and air-dried. The precursor materials are designated CrZrP12, CrZrP17, CrZrP25, and CrZrP34, where the figures correspond to the basal spacings determined by powder XRD. (The basal spacings for powdered samples are lower than those obtained on the films reported in ref 8). CrZrP34 was calcined at 400 °C (CrZrP400)

[†] Université Montpellier 2.
[‡] Universidad de Malaga.
[§] ICMAT-CNR, Rome.
[⊗] Abstract published in *Advance ACS Abstracts,* July 15, 1995.

(1) (a) Burch, R. *Catal. Today, Pillared Clays* **1988**, *2* (2−3). (b) Pinnavaia, T. J. *Science* **1983**, *220*, 365.
(2) (a) *Expanded Clays and Other Microporous Solids*, Occelli, M. L., Robson, H. E., Eds.; Van Nostrand: New York, 1992. (b) Tomlinson, A. A. G. In *Pillared Layered Structures. Future Trends and Applications*; Mitchell, I. V., Ed.; Elsevier: Amsterdam, 1990; p 91.
(3) Pinnavaia, T. J.; Tzou, M. S.; Landau, S. D. *J. Am. Chem. Soc.* **1985**, *107*, 4783.
(4) (a) Tzou, S.; Pinnavaia, T. J. In ref 1, p 243. (b) Skoularikis, N. D.; Caughlin, R. W.; Kostapapas, A.; Carrado, K. A.; Suib, S. L. *Appl. Catal.* **1988**, *39*, 61. (c) Choudary, B. M.; Prasa, A. D.; Bhuma, V.; Swapna, V. *J. Org. Chem.* **1992**, *57*, 5841. (d) Martin, K. Thesis, Univ. Wales, 1986.
(5) Maireles-Torres, P.; Olivera-Pastor, P.; Rodriguez-Castellon, E.; Jimenez-Lopez, A.; Tomlinson, A. A. G. In *Multifunctional Mesoporous Inorganic Solids*; Hudson, M. J., Sequeira, C. A. C., Eds.; NATO ASI Ser. Vol. 400; Kluwer Academic: Dordrecht, The Netherlands, 1993; p 237.
(6) Cleafield, A.; Kuchenmeister, M. in *Supramolecular Architecture in Thin Films and Solids*; Bein, T., Ed.; ACS Symp. Ser. Vol. 299; American Chemical Society: Washington, DC, 1993, p 128.
(7) Bornholdt, K.; Corker, J. M.; Evans, J.; Rummey, J. M. *Inorg. Chem.* **1991**, *30*, 1.
(8) (a) Maireles-Torres, P.; Olivera-Pastor, P.; Rodriguez-Castellon, E.; Jimenez-Lopez, A.; Tomlinson, A. A. G. *J. Mater. Chem.* **1991**, *1*, 319. (b) *Ibid. J. Solid State Chem.* **1991**, *94*, 368.

0020-1669/95/1334-4611$09.00/0

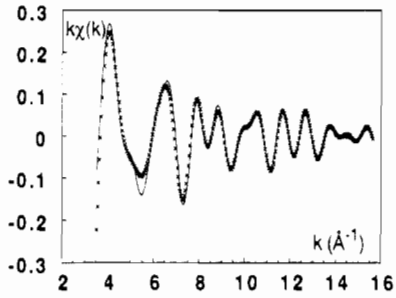

Figure 1. XAFS spectrum of α-Cr_2O_3 (Fourier filtered up to 4 Å, ×) and that calculated (—) using the structural parameters of Table 1.

and at 800 °C (CrZrP800) under nitrogen to provide chromia-pillared derivatives. The experimental conditions and chemical analyses of the materials were as described previously.[8]

X-ray Absorption Spectroscopy (XAS). XAS spectra of solid samples were recorded at the Cr K-edge at 77 K in the transmission mode using a cold finger cryostat on station 8.1 of the SRS, SERC Daresbury Laboratory, Daresbury, U.K., typical beam conditions being 2 GeV and 150 mA. The spectrometer was equipped with a Si(111) double crystal monochromator slightly detuned for harmonic rejection. Solid samples of precursor and calcined samples, diluted as necessary with boron nitride, were prepared as Nujol mulls pressed between the Parafilm windows of aluminium sample cells. Samples prepared in this way are homogeneous, free from pinholes or cracks. Calibration was carried prior to all measurements using a 5 μm Cr foil, defining the first inflection point in the edge as 5989 eV. The XAS spectrum of α-Cr_2O_3 (Merck, 99% purity) was recorded under the same conditions. This compound was used to test the transferability of McKale *ab initio* calculated phase and amplitude functions[9] and for comparison of near-edge regions.

Spectra were recorded from *ca.* 200 eV before the edge to 900 eV after, in series of step sizes and counting times within energy regions corresponding to pre-edge, edge, and three post-edge regions. The ionization chambers I_o and I_T were filled with argon/helium mixtures (I_o, 2% Ar; I_T, 15% Ar; total pressure in both chambers is atmospheric).

Data Analysis. Data analysis was carried out utilizing the programs of Michalowicz.[10] XAFS spectra were extracted after first subtracting a straight line or Victoreen pre-edge from the entire spectrum and removing the absorbing atom background *via* spline polynomials. Fourier transformation (FT) (Kaiser window) was carried out over the *k*-range 2.5−15 $Å^{-1}$. In a first stage, maxima in the FT were individually filtered over appropriate *R*-ranges and back-transformed into *k*-space, and the XAFS functions obtained were fitted using the single-scattering, small-atom approximation. Subsequently, broader Fourier filter envelopes allowed curve fitting over regions corresponding to 1−4 Å in direct space. The value of the term γ (the mean free path of the photoelectron, λ, is equal to k/γ), used in refinements of XAFS spectra of the precursor and calcined phases, was derived from curve fitting of α-Cr_2O_3. The energy offset, ΔE_o, was varied with each shell fitting.

Below 3.7 Å, α-Cr_2O_3 has five coordination shells[11] which give rise to three maxima in the Fourier transformed XAFS spectrum: 6 oxygens at 1.99 Å ; 1 and 3 chromium atoms at 2.65 and 2.89 Å, respectively; 3 and 6 chromium atoms at 3.43 and 3.66 Å, respectively. As shown in Figure 1, all the features in the XAFS spectrum can be reproduced satisfactorily in this formalism and using *ab initio* phase and amplitude functions. Interatomic distances derived from XAFS are within 0.01 Å of the crystallographic values, Debye−Waller type factors lie in the range 0.05−0.07 Å, and the γ values are close to unity for both oxygen and chromium backscatterers. These results, summarized in Table 1, indicate the suitability of the single scattering approximation for the XAFS analysis of this type of system and the transferability of the phase and amplitude functions.

The goodness of fit between experimental and calculated spectra is expressed in each case as the residue res = $\sum_k(k[\chi_{expt}(k)] - k[\chi_{calc}(k)])^2k^3/\sum_k(k[\chi_{expt}(k)]^2)k^3$.

Results and Discussion

***K*-Edge Spectra.** Figure 2a,b shows the Cr K-edge spectra in the XANES region of the CrZr17 and CrZrP34 precursors, Figure 2c,d the near-edge region of CrZr400 and CrZr800, respectively, and Figure 2e that of reference Cr_2O_3. The other precursors gave virtually identical K-edge spectra in the energy range to 6100 eV. All compounds show a low intensity pre-edge feature at 5989 eV, while the oxide samples present, in addition, a second pre-edge feature at slightly higher energy and a well-defined inflection point in the absorption edge. The low-intensity pre-edge features are characteristic of *ca.* O_h CrO_6 moieties; in particular, in no case was there any evidence for the presence of enhanced intensity pre-edge features, as would be expected for asymmetric (T_d or five-coordinate) sites[12] and observed, for example, in $K_2Cr_2O_7$ (Figure 1f) and $SrCrO_4$.[13] The multiple scattering effects seen at and above the absorption edge (energy range 6000−6030 eV) of Cr_2O_3 are absent in chromia-pillared samples CrZr400 and CrZr800, providing first evidence of more restricted long-range order in the latter two.

XAFS Analysis. Polyhydroxychromium(III) Precursors. The Fourier transformed XAFS spectra (FT) of the precursor materials are shown in Figure 3. Of the four precursors examined, CrZrP17 and CrZrP34 gave results most clearly interpretable in geometrical terms and will be discussed first. The two maxima in the FTs of these samples, Figure 3a, were identified in a first stage, by making use of the Lee−Beni criterion,[14] as resulting from backscattering from oxygen and chromium atoms, respectively.

For CrZrP17, the result of curve fitting in *k*-space is in agreement with a first coordination shell of 6 oxygen atoms at 1.97(2) Å and a second shell of 2 chromium atoms at 3.06 Å. Among the various oligomeric species the dimer, although it would give a single distance in XAFS, can be rejected on the basis of the incompatibility of the coordination number (1) with that observed for CrZrP17 (2). In fact the only condensed species that would produce in XAFS both a single metal−metal distance and a coordination number of 2 is a geometry based on a cyclic trimer. Nonlinear trimers have been identified in the solid state by X-ray diffraction. For example, in $Cr_3(OAc)_6OCl.5H_2O$,[15] the chromium atoms are linked through a central oxygen and *via* acetate groups, an arrangement which gives a Cr- - -Cr distance of 3.28 Å, longer than that observed here. The Cr_3 cluster in $[Cr_3(NH_3)_{10}(OH)_4]Br_5.3H_2O$[16] is linked on two edges through bridging OH groups (Cr- - -Cr = 3.61 Å) and on the third *via* a double hydroxide bridge, where the interatomic distance between chromium atoms is 2.995 Å. In general terms, from consideration of a number of structures containing trimeric and tetrameric chromium[17] units,[15-18] those linked *via* single OH or oxo bridges have bond lengths *ca.* 3.6 Å, while those having a double oxo or hydroxy bridge are characterized by Cr- - -Cr separations of *ca.* 2.9−3 Å. The various trimer and tetramer species put forward from potentiometric and optical studies as being the most probable

(9) McKale, A. G. *J. Am. Chem. Soc.* **1988**, *110*, 3763.
(10) Michalowicz, A. In *Logiciels pour la Chimie*; Société Française de Chimie: Paris, 1991; pp 102−103.
(11) Newnham, R. E.; de Haan, Y. M. *Z. Krist.* **1962**, *117*, 235.
(12) (a) Durham, P. J.; Pendry, J. B.; Hodges, C. H. *Solid State Commun.* **1981**, *38*, 159. (b) Sainctavit, P.; Petiau, J.; Benfatto, M.; Natoli, C. R. *Physica B* **1989**, *158*, 347.
(13) Gibb, T. C. *J. Mater. Chem.* **1992**, *2*, 105.
(14) Lee, P. A.; Pendry, J. B. *Phys. Rev. B* **1975**, 2795.
(15) Figgis, B. N.; Robertson, G. B. *Nature* **1965**, *205*, 694.
(16) Andersen, P.; Damhus, T.; Pedersen, E.; Petersen, A. *Acta Chem. Scand.* **1984**, *A38*, 359.
(17) Bang, E. *Acta Chem. Scand.* **1984**, *A38*, 419.
(18) Andersen, P.; Bang, E. *Acta Chem Scand.* **1986**, *A40*, 476.

Table 1. Structural Parameters of Precursors and Chromia Pillared Zirconium Phosphate Materials Determined by X-ray Absorption Spectroscopy[a]

	CrZrP17 (res 5%)			CrZrP34 (res 4%)		
atom	R^{XAS}	N	σ	R^{XAS}	N	σ
$Cr-O_{short}$	1.97	6	0.055	1.98	6	0.065
Cr−Cr1				2.95	0.8	0.027
Cr−Cr2	3.06	2	0.052	3.08	1.5	0.037
Cr−Cr3				3.65	1.5	0.032
$Cr-O_{long}$	3.67	2	0.069	3.75	4	0.012

	α-Cr_2O_3 (res 5%)				CrZrP400 (res 4%)			CrZrP800 (res 5%)		
atom	$R^{X\text{-}ray}$	R^{XAS}	N	σ	R^{XAS}	N	σ	R^{XAS}	N	σ
Cr−O	1.99	1.99	6	0.066	2.00	6	0.077	2.00	6	0.077
Cr- - -Cr1	2.65	2.67	1	0.066	2.67	0.2	0.040			
Cr- - -Cr2	2.89	2.90	3	0.049	2.95	5	0.11			
Cr- - -P					3.25	0.3	0.02	2.70	0.6	0.02
Cr- - -P								3.10	1.5	0.02
Cr- - -Cr3	3.43	3.42	3	0.059						
Cr- - -O_{long}								3.49	7	0.01
Cr- - -Cr4	3.66	3.65	6	0.060				3.71	2.5	0.02

[a] R^{XAS} interatomic distance determined from XAS, esd ± 0.02 Å; $R^{X\text{-}ray}$ interatomic distance determined crystallographically;[11] N = number of nearest neighbors, esd 20%; σ = Debye−Waller factor in Å esd 0.005.

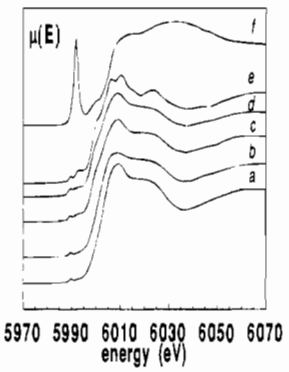

Figure 2. Near-edge region of precursor phases CrZrP17 (a) and CrZrP34 (b) and calcined phases CrZrP400 (c), CrZrP800 (d), Cr_2O_3 (e), and $K_2Cr_2O_7$ (f).

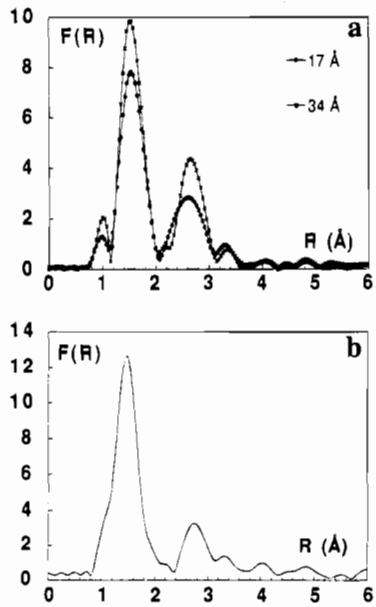

Figure 3. Comparison of Fourier transformed XAFS spectra of chromia pillar precursor phases with interlayer distances 17 and 34 Å (CrZrP17, CrZrP34) (a) and 12 Å (CrZrP12) (b).

species of higher connectivity existing in aqueous solution[19] are shown in Scheme 1. The Cr- - -Cr distance derived from XAFS for CrZrP17 agrees with their linking through a double hydroxide bridge, and the most likely arrangement is that containing a $Cr_3(\mu\text{-}OH)_4$ unit, shown to be highly stable in acidic solution.[20]

The first peak in the FT of CrZrP34 (obtained using higher Cr/Zr ratio solutions[8]) again corresponds to 6 oxygen atoms at 1.98 Å. However, curve fitting in reciprocal space remained unsatisfactory unless the second maximum in the FT was considered to be composite, with contributions from two shells of chromium atoms, at 2.95 and 3.08 Å. Furthermore, an additional shell of chromium atoms included at *ca.* 3.6 Å gave a significantly improved fit. The corresponding coordination numbers determined by XAFS are 0.8, 1.5, and 1.5 Cr atoms, respectively.

The first and third Cr- - -Cr distances are consistent with the presence of a local environment such as that drawn in Figure 4, in which the distances between chromium atoms linked through a double OH bridge and through a single OH bridge are 2.95 and 3.65 Å, respectively. This cluster has been suggested as a general intermediate in the process of condensation to trimers, tetramers, *etc.* in aqueous Cr^{3+} solutions.[21] The second distance derived from XAFS analysis, 3.08 Å, is similar to that observed in the cyclic trimer. Taken together, these observations are consistent with the presence of an oligomer of connectivity **2** of Scheme 1 and are in agreement with a sequential condensation process leading from the trimer to an open tetramer.[21]

Equilibria between more or less highly condensed tetramers of charge 5+, 6+, or 8+ exist in solution depending upon the ambient pH. In the present case, the XAFS results suggest that **2** is intercalated in preference to the closed tetramer **3** (which has no single OH bridges and hence no Cr- - -Cr distances of 3.65 Å), a process which is presumably favored by the low pH of the solution and the high charge density on the phosphate layer. A different open tetramer **5** that may be considered to be derived from **4** by hydrolysis of two of the singly bridging OH groups has recently been identified using XAFS in a bentonite contacted with chromium nitrate solution.[7] Cr- - -Cr

(19) (a) Spiccia, L.; Stoeckli-Evans, H.; Marty, W.; Giovanoli, R. *Inorg. Chem.* **1987**, *26*, 474. (b) Stünzi, H.; Spiccia, L.; Rotzinger, F. P.; Marty, W. *Inorg. Chem.* **1989**, *28*, 66 and references therein. (c) Stünzi, H.; Rotzinger, F. P.; Marty, W. *Inorg. Chem.* **1984**, *23*, 2160.
(20) Spiccia, L.; Marty, W.; Giovanoli, R. *Inorg. Chem.* **1988**, *27*, 2660.
(21) (a) Stünzi, H.; Marty, W. *Inorg. Chem.* **1983**, *22*, 2145. (b) Manceau, A.; Charlet, L. *J. Colloid Interface Sci.* **1992**, *148*, 425.

Scheme 1. Trimeric and Tetrameric Polyhydroxychromium(III) Species

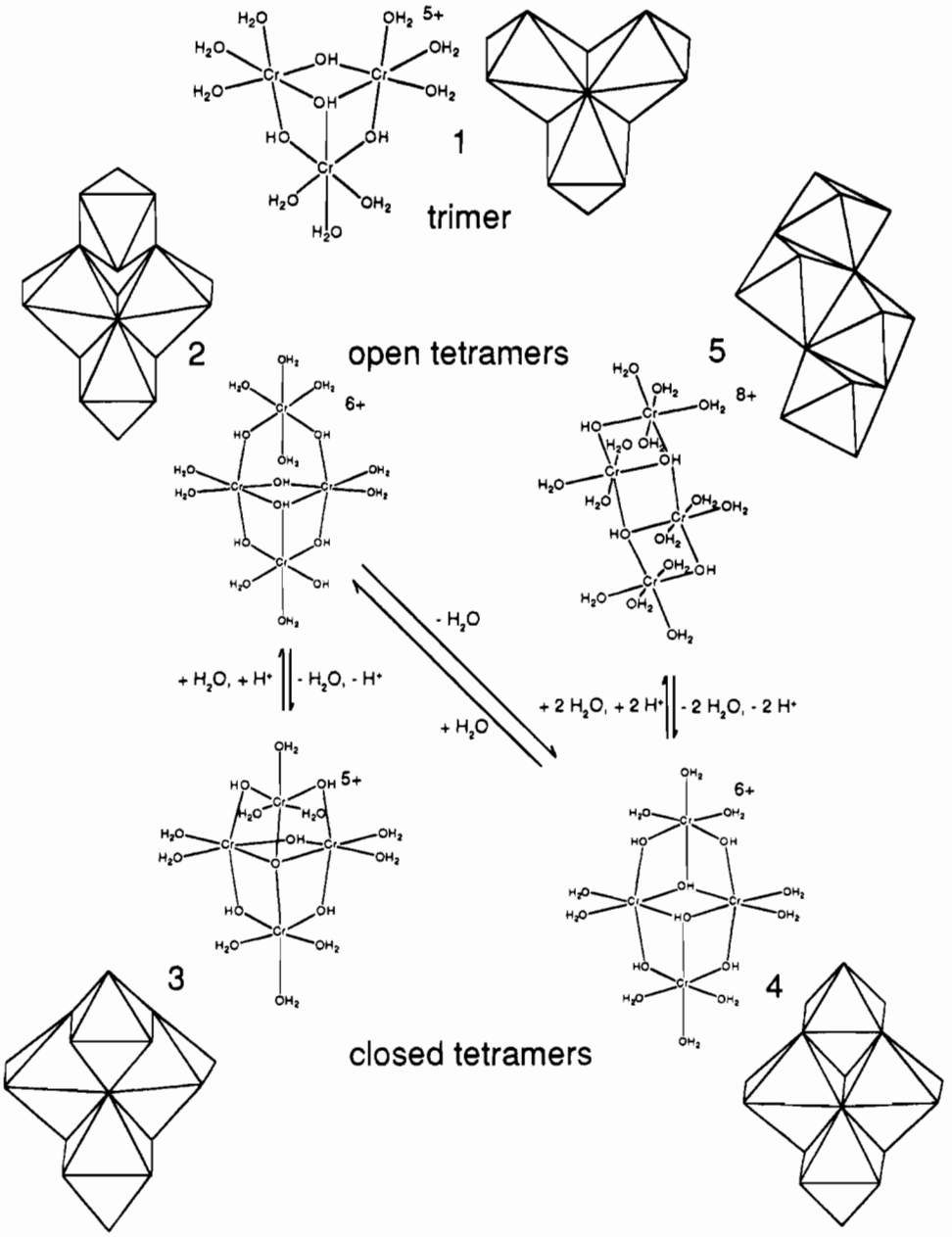

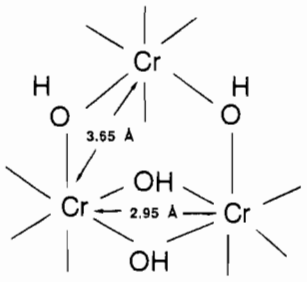

Figure 4. Common structural fragment in the condensation processes leading to oligomeric polyhydroxochromium(III) species.

distances in this precursor are 2.97 (2 Cr) and 3.90 Å (2 Cr). It is inferred that the nature of the oligomeric species intercalated in bentonite and zirconium phosphate—more highly condensed and less highly charged in the latter—results from the different method of preparation of the pillaring solution and, possibly, from the different charge densities on the host layered solids.

For CrZrP17 and CrZrP34, the final fits between the Fourier filtered spectrum and that calculated using the XAFS equation are shown in Figure 5 and the corresponding structural parameters are collected in Table 1.

We now turn to the XAFS analysis of CrZrP12 and CrZrP25. The former has an increase in basal spacing of only *ca.* 5.5 Å compared with anhydrous ZrP, and the possibility of insertion of a $Cr(H_2O)_6^{3+}$ monomer thus arises (expected expansion *ca.* 5 Å). XAFS analysis clearly shows this not to be the case, since, in addition to the CrO_6 first shell having Cr−O = 1.97(2) Å, chromium atoms occupy the second coordination shell.

Arriving at a satisfactory fit for the CrZrP25 Å proved more complicated. Cr- - -Cr shells at distances corresponding either exclusively to the trimer or the possible tetramer clusters of Scheme 1 provided unsatisfactory agreement. Instead, the XAFS could be reasonably fitted only by parameters lying between the two, with the implication that both tri- and tetranuclear clusters are present. We recall that uptake from a very high Cr^{3+}/Zr phosphate ratio mixtures decreases,[8] which could be interpreted in terms of a modification of the selectivity of the phosphate surface to attaching species.

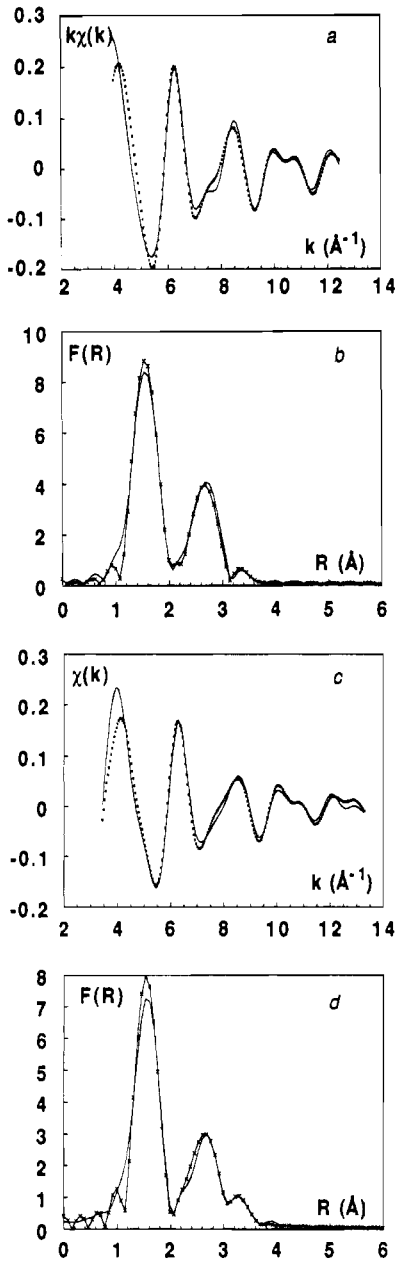

Figure 5. Comparison in *k*-space (a, c) and *R*-space (b, d) of the experimental curve (×) and that calculated (—) for CrZrP17 (a, b) and CrZrP34 (c, d) using the structural parameters of Table 1.

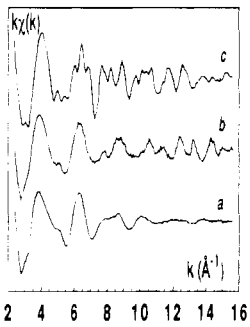

Figure 6. XAFS spectra of CrZrP400 (a), CrZrP800 (b), and Cr_2O_3 (c).

Several other points are of note as regards these connectivities. First, for all materials, the residual OAc groups appear to have little (if any) influence on the XAFS analysis. As a consequence, it is not possible to choose between a simple intercalation mechanism or the anchoring mechanism put forward previously to rationalize formation of porous materials in this system.[8] Second, using the dimensions of trimeric and tetrameric chromium oligomers, estimated from crystallographic studies,[15-18] interpretation in terms of their orientation and the eventual formation of multilayers within the interlayer region of zirconium phosphate can be considered. The trimer, with a depth of *ca.* 5 Å and a length of 6.5 Å, would produce in zirconium phosphate interlayer distances of 11.5 or 13 Å for insertion parallel or perpendicular to the layers, respectively. On this basis, the observed expansion of 11 Å for CrZrP17 is most compatible with a double layer of parallel oriented trimers. For the 34 Å phase, the free height of *ca.* 27 Å implies that at least a double layer of tetramers (length *ca.* 10 Å, depth *ca.* 6.5 Å) must be intercalated, with water molecules of this highly hydrated sample occupying the remaining interlayer space. Conversely, the free height of only *ca.* 5.5 Å for CrZrP12 would be consistent with a dimer species aligned perpendicular to the phosphate layers. Few pillaring studies have been concerned with such low-free height materials, but they—including the present example—should provide clearer correlation with porosity models.

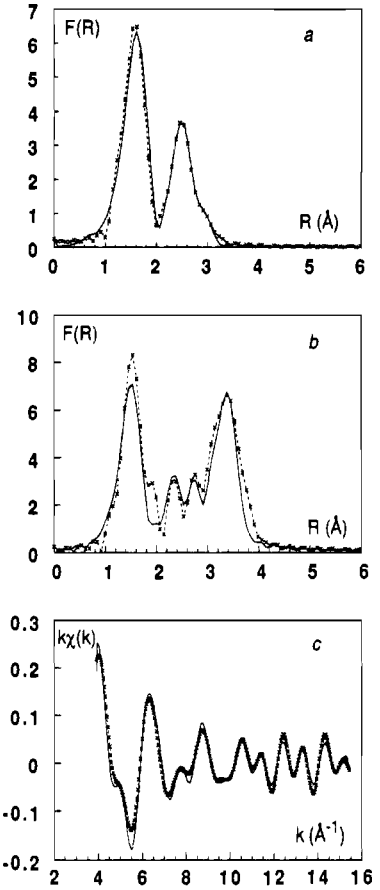

Figure 7. Comparison of the experimental Fourier transformed spectra (×) and those calculated (—) using the values in Table 1 for CrZrP400 (a) and CrZrP800 in *R*-space (b) and *k*-space (c).

Finally, the absence of multiple-scattering effects in the clusters of higher connectivity (expected for linear—or almost linear—arrays of Cr atoms[22]) indicates that there are no wholesale rearrangements of Cr clusters on surface attachment.

A comparison is now possible with a recent study of individually prepared polyhydroxy–Cr^{III} oligomers (*via* chromatography) intercalated into montmorillonite (albeit by a different process).[23] In that study, it was found that the clusters

(22) Teo, B. K. *EXAFS Spectroscopy, Basic Techniques and Data Analysis*; Springer Verlag: Berlin, 1986.

retained their connectivities on intercalation but that concomitant expansions were low and compatible with the insertion of single layers: 5.5 Å (parallel oriented trimer) and 6.7 and 6.5 Å (open and closed tilted tetramers). Differences with the present work underline the importance of both the strongly directing tendency of pendant −POH groups and the flat surface of the α-structured metal(IV) phosphates as compared with the hexagonal pocket surface of montmorillonite. It also provides support for a more orderly growth on the colloid surface adopted.

Chromia-Pillared Forms. The calcined forms examined, CrZrP400 and CrZrP800, are both derived from the 34 Å precursor and were chosen because they represent materials with the highest specific surface area and free height. The Cr *K*-edge of these materials and that of Cr_2O_3 and several precursor materials for comparison are shown in Figure 2. Apart from detail at 6000−6005 eV in Cr_2O_3 due to the influence of Cr atoms beyond the 3rd shell,[22] the spectra of Cr_2O_3 and CrZrP400 are substantially the same, implying that they have a similar geometry. Also, there is little evidence either for enhanced Cr *K*-near-edge absorption or shift in edge position on calcination; *i.e.* there are no gross changes in oxidation state or geometry.

XAFS analysis was carried out in the standard way for Cr_2O_3, and extracted parameters are listed in Table 1; they compare well with literature crystallographic values.[11] Above 3 $Å^{-1}$, the XAFS oscillations in CrZrP400 are more rapidly damped than those in the 800 °C congener, indicating less long-range ordering. For the former, analysis of the first two maxima in the FT was relatively straightforward, with the second identified as resulting from two chromium shells at 2.67 and 2.95 Å. To this point, the local structure around chromium in the pillar of CrZrP400 is a fragment of that in Cr_2O_3. However, there was significant improvement in simulation and fit when a small contribution from distant P atoms was included. Observation of phosphorus atoms at 3.25 Å provides direct evidence that the "chromia" particles are attached directly to the phosphate layer through Cr−O−P−O− linkages. Making use of this distance and bond lengths for Cr−O and P−O of 2.0 and 1.5 Å, respectively, allows a Cr−O−P bond angle of 135° to be calculated. This is the first structural evidence for crosslinking, although previous studies of these materials by X-ray photoelectron spectroscopy showed an increment in the binding energy of P_{2p} and Zr_{3d} indicating the possible formation of a covalent pillar to layer bond.[24] Further, the fact that there is no third, "Cr_2O_3-type", Cr- - -Cr shell provides strong evidence that the nano-oxide pillar is highly anisotropic (each chromium atom experiences fewer lateral neighbors than would be the case for a more spheroidal particle). In addition, the absence of multiple scattering effects provides further evidence that the arrangement of Cr atoms is not linear. (This also means that Cr- - -Zr distances are unobservable, so no information is available on this aspect.) Taken together, with recollection that the 400 °C calcined form has a free height of 19.5 Å, the results suggest the presence of a ribbonlike pillar as in Scheme 2, derived *via* condensation of bilayers of the open tetramer precursor **4** (Scheme 1).

CrZrP800 is X-ray amorphous with a BET surface area of *ca.* 200 $m^2 g^{-1}$. Attempts to simulate the XAFS of this calcined phase utilizing two shells of chromium atoms beyond the first oxygen octahedron were unsuccessful. Fits were possible only when the two shells present in the range 2.6−3.2 Å were both assigned as arising almost entirely from Cr- - -P contributions,

Scheme 2. Ribbon Structure of Chromia Pillars in CrZrP400 Consistent with the XAFS Result

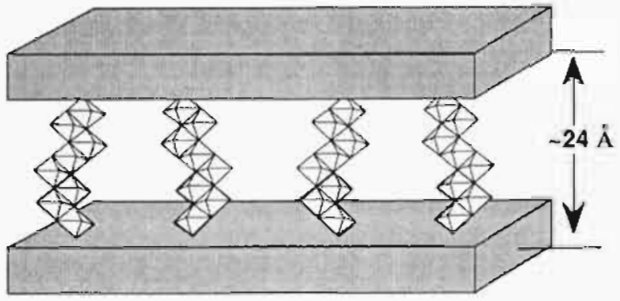

with backscattering from chromium and oxygen atoms at 3.7 and 3.5 Å, respectively. This sequence of coordination shells is very similar to that in $CrPO_4$ both in atom type and interatomic distance; in α-$CrPO_4$,[25] phosphorus lies at 2.68 and 3.21 Å from chromium, and Cr- - -Cr and Cr- - -O distances both have mean values of *ca.* 3.5 Å. The oscillations of the XAFS spectrum of this calcine are well-defined beyond 12 $Å^{-1}$, unlike the damped signal given by CrZrP400. This observation is in agreement with a structural modification of the oxidic pillar, which has acquired a considerable phosphate "outer coating". One possible interpretation lies in terms of a partial collapse of the ribbon structure, with a concomitant increased contact between the pillar and the phosphate matrix in CrZrP800 than in CrZrP400. Alternatively, redistribution of phosphate groups from the layer to the pillar would imply that the phosphate layers have also undergone some degradation,which is accompanied by the onset of chromium phosphate formation, either in the form of interlamellar nanoparticules or as an amorphous bulk phase. This is an intermediate amorphous structure between the ordered pillared materials at 400 °C and the products formed after calcination of the sample under air or nitrogen at 1000 °C, where ZrP_2O_7 and Cr_2O_3 are clearly detected by XRD.

Other spectroscopic methods were used in attempts to provide complementary evidence for these formulations. ^{31}P MAS NMR might be expected to provide information on the evolution of the phosphorus environment in going from the precursor to the calcined phases, as in the formation of silica pillars from precursor intercalated ZrP.[26] However, the presence of chromium broadens the resonance lines, and both the precursor CrZrP34 and CrZrP400 give signals centered at −20.5 ppm (relative to H_3PO_4), a slight upfield shift from the resonance at −18.7 ppm in pristine ZrP. EPR spectra are of little diagnostic use, both precursors and "chromia"-containing materials giving characteristic Cr^{3+} signals with a *g* factor of 1.98. However, the optical spectra are more informative, the precursors showing no evidence of the presence of Cr^{VI}, although no distinction can be drawn between the various samples. Chromia-pillared materials give more ambiguous spectra, with changes observed with respect to simple CrO_6 chromophores, Figure 8. The absence of characteristic $Cr^{VI}O_4$[27] supports the XAFS results.

In the infrared spectra, recorded over the region 400−4000 cm^{-1}, a broadening and splitting of the $\nu_3(PO_4)$ mode in going from ZrCrP400 to CrZrP800 is seen, as expected for coordination of bidentate PO_4^{3-} groups in the latter.

The literature contains several examples of intercalative registry changes, ranging from small-molecule reorientation (a

(23) Drljaca, A.; Anderson, J. R.; Spiccia, L.; Turney, T. W. *Inorg. Chem.* **1992**, *31*, 4894.
(24) Guerrero-Ruiz, A.; Rodriguez-Ramos, I.; Fierro, J. L. G.; Jimenez-Lopez, A.; Olivera-Pastor, P.; Maireles-Torres, P. *Appl. Catal.* **1992**, *92*, 81.
(25) Attfield, J. P.; Sleight, A. W.; Cheetham, A. K. *Nature* **1986**, *322*, 620.
(26) Cassagneau, T.; Jones, D. J.; Rozière, J. To be published.
(27) Lever, A. B. P. *Inorganic Electronic Spectroscopy*, 2nd ed.; Elsevier: Amsterdam, 1984.

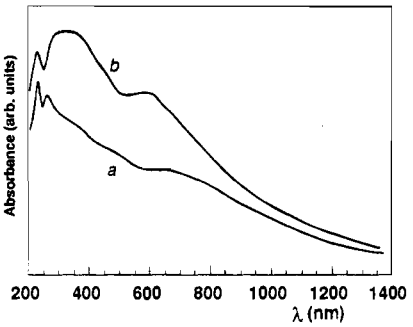

Figure 8. Optical spectra of CrZrP400 (a) and CrZrP800 (b).

recent example is that between Na^+ and NH_3 in TiS_2[28]) to complex-chemistry type interactions.[29] However, they all involve noncovalently linked species, i.e. species retaining a considerable degree of freedom between the layers. Similarly, theoretical models of layer rigidity after pillaring have concerned organoclays,[30] in which there is still intralamellar space for "pillar" reorientation. A chemical rather than physical model must be suggested to rationalize these results. For zirconyl and alumina pillars there is evidence that exchangeable pillar OH groups[31] remain important even at 400 °C.

The pillar structure consistent with the XAFS results depicted in Scheme 2 is different from that suggested for chromia-pillared bentonite,[7] for reasons attributed to the method of synthesis and the character of the host solid. These examples serve in addition to underline the usefulness of the X-ray absorption technique, capable of providing precise information allowing differences in the nature both of the oligomeric polyhydroxychromium(III) species and of the corresponding pillaring oxidic fragments produced on calcination to be discerned and described in structural terms.

Conclusions

This attempt to determine the pillar structure in a pillared layered solid demonstrates that, in favorable circumstances (if a transition metal is present in the pillar and if the layered matrix is suitable, i.e. does not contain very high-Z atoms), XAS is capable of providing considerable insight into the pillaring process. In addition, it has shown that (i) the pillar at 400 °C is indeed a Cr^{III} oxide nanoparticle, best described as a modified fragment of chromium oxide bound through Cr−O−P interactions to the metal phosphate layer and (ii) despite the complex reaction with the layer at 800 °C, a porous pillared material is still present. More extensive work is underway on other examples which we hope will enable correlations to be made between pillar structure and porosity models.

Acknowledgment. We thank Dr. Bernard Mula for his contribution to the preparation of this manuscript, the Commission of the European Communities (Brite-EuRam projects I-0027 and BRE2-CT93-0450) and the CICYT (Spain, Project No. MAT94-0678) for financial support, and the Daresbury Laboratory, Daresbury, U.K., for access to the SRS though the European Large Facilites programme. P.M.-T. was supported by a personal bursary under Brite-EuRam ERB.BRE2.CT93.3005.

IC9501733

(28) Burr, G. L.; McKelvy, M. J.; Glaunsinger, W. S. *Chem. Mater.* **1993**, *5*, 1363.
(29) Ferragina, C.; Massucci, M. A.; Patrono, P.; La Ginestra, A.; Tomlinson, A. A. G. *J. Phys. Chem.* **1985**, *89*, 4762.
(30) Kim, H.; Jin, W.; Lee, S.; Zhou, P.; Pinnavaia, T. J.; Mahanti, S. D.; Solin, S. A. *Phys. Rev. Lett.* **1988**, *60*, 2168.
(31) Dyer, A.; Gallardo, D. In *Recent Developments in Ion Exchange 2*, Williams, P. A., Hudson, M. J., Eds.; Elsevier: Amsterdam, 1990; p 75.